Pergamon

Phys. Chem. Earth (C), Vol. 26, No. 7, pp. 513–517, 2001
© 2001 Elsevier Science Ltd.
All rights reserved
1464-1917/01/$ - see front matter

PII: S1464-1917(01)00039-3

Competition Between Two- and Three-Body Decay of Cl_2O

M. Roth, T. Einfeld, K. -H. Gericke and C. Maul

Institute of Physical and Theoretical Chemistry, University Braunschweig, Germany

Received 14 June 2000; accepted 15 November 2000

Abstract. The photodissociation dynamics of Cl_2O at 235nm and 207nm are investigated. The chlorine atoms generated via dissociation into the radical and three-body decay channel are detected state specifically in a (2+1)-REMPI process. At 235nm the Cl_2O molecule was excited to the 1^2B_1 state and the decay is dominated by the radical dissociation $Cl_2O+h\nu \rightarrow ClO+Cl$. At 207nm an excitation into the 2^1A_1 state takes place, which dissociates predominantly into the three-body channel $Cl_2O+h\nu \rightarrow 2Cl+O$. The three-body decay is characterized based on the fragment kinetic energy distributions at 235nm and 207nm. The shape of the energy distributions points to an asynchronous concerted decay mechanism. © 2001 Elsevier Science Ltd. All rights reserved

1 Introduction

Due to the fundamental significance of elementary three-body processes, e.g. in the ozone formation process $O+O_2+M \rightarrow O_3+M^*$, it is somewhat surprising that even for photo induced three-body decay processes as their simplest example only relatively few studies exist leaving uncharted territory in the map of physical chemistry. We have investigated the three-body decay of phosgene ($COCl_2$), thionyl chloride ($SOCl_2$) and dichloromonoxide (Cl_2O) (Maul et al., 1997; Maul and Gericke, 2000) using REMPI/TOF measurements (resonance enhanced multi-photon ionisation/time of flight). Emphasis is laid on the distinction between concerted and stepwise processes, consisting of one single or two consecutive kinetic events, respectively. If a molecule ABC dissociates into its atomic fragments A, B, and C, the bondbreaking processes can take place in unison or not.

$$ABC + h\nu \xrightarrow{t_0} ABC^* \xrightarrow{t_1} AB^* + C \xrightarrow{t_2} A + B + C \qquad (1)$$

Correspondence to: M. Roth, m.roth@tu-bs.de

The decay is called sequential for a time difference $\Delta t=t_2-t_1$ being greater than the rotational period τ_{rot} of the intermediate AB. If it is smaller, the dissociation is denoted as concerted. Concerted fragmentation is further classified as either synchronous ($\Delta t \approx 0$) or asynchronous ($0<\Delta t<\tau_{rot}$). This classification is of special importance to atmospheric chemistry, since secondary collision processes may influence the final products depending on whether the decay proceeds in a stepwise or synchronous manner. The different mechanisms produce different specific fragment energy distributions, which in turn can be used to study the decay dynamics by sensitive detection techniques like REMPI/TOF.

Here we present the results for Cl_2O as an example of one of the simplest fragmentation processes with respect to three atomic products. The photodissociation of Cl_2O might follow three different dissociation channels. One is the two-body decay into ClO and Cl (eq.(2)), which is named radical decay, one is the fragmentation into Cl_2 and O (eq.(3)), the molecular channel, and there is the three-body decay into two chlorine atoms and one oxygen atom (eq.(4)).

$$Cl_2O + h\nu \rightarrow ClO + Cl \quad \lambda_{thresh} = 868\text{nm} \qquad (2)$$

$$+ h\nu \rightarrow Cl_2 + O \quad \lambda_{thresh} = 729\text{nm} \qquad (3)$$

$$+ h\nu \rightarrow 2Cl + O \quad \lambda_{thresh} = 297\text{nm} \qquad (4)$$

In previous studies of the photodissociation of Cl_2O at 248nm and 308nm (Nelson et al., 1994; Moore et al., 1997), the dominating dissociation channel was found to be the radical channel. At 193nm the three-body channel is the main dissociation channel (Nelson et al., 1994). From the absorption cross section of chlorine monoxide shown in fig.1 it is evident that the molecule is excited into different electronic states depending on the excitation wavelength. From the previous studies and the assignment of excited electronic states of Cl_2O, we assume the three-body decay to dominate for photolysis

wavelengths below 220nm. Therefore we performed photolysis experiments at both sides of the absorption minimum at 220nm, repeating previous sudies by Tanaka et al. (1998) at 235nm and comparing the results to data obtained for the unknown wavelength of 207nm.

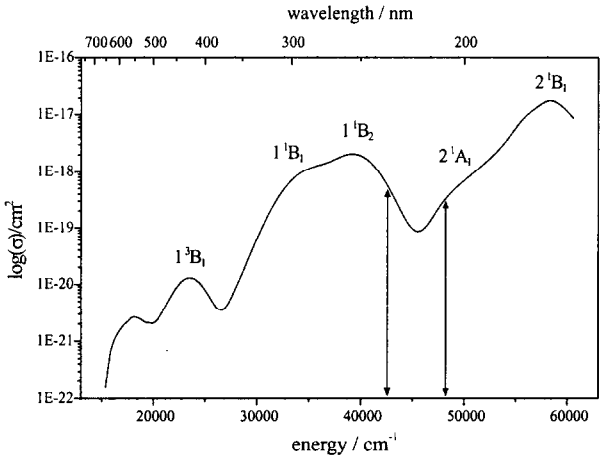

Fig. 1. Logarithmic absorption cross section of Cl_2O based on the publications of Nee (1991), Lin (1976) and DeMore et al. (1997). The assignment of the electronic states is taken from the calculations of Nickolaisen et al. (1996). The wavelengths used in the present experiment are marked by arrows.

2 Experimental

The linear time of flight spectrometer is described in details elsewhere (Haas et al., 1993). Basically it consists of a stainless steel tube evacuated to a base pressure of 10^{-4}Pa equipped with quartz windows for photolysis and probe lasers traversing perpendicular to the single field TOF spectrometer. The Cl_2O molecules were generated according to the method of Cady (1957) and purified from chlorine molecules by a vacuum distillation. The Cl_2O gas (80-130$\times 10^2$Pa) was mixed with argon to a total pressure of 10^5Pa. A pulsed nozzle (General Valve Series 9) was used to expand the gas mixture inside the spectrometer perpendicular to the spectrometer axis. Using repetition rates of 10Hz and a stagnation pressure of 2-10$\times 10^4$Pa we obtained a background pressure of about 10^{-2}Pa with the nozzle in operation. An excimer pumped dye laser system (Lambda Physik LPX 100, Lambda Physik LPD 3000) was used to generate radiation at 470nm and a Nd:YAG laser pumped dye laser (Coherent Infinity 40-100, Lambda Physik Scanmate) delivered 414nm radiation. Both lasers were frequency-doubled by two different BBO crystals. The energy of the frequency-doubled light amounted to 200-600μJ per pulse. The laser beam at 235nm was focussed with a lens of 90mm focal length, while at 207nm a lens of 150mm focal length was used. The laser beams were collinear but counter propagating and ultimate care was taken to overlap the focal points. The timing between the lasers and the molecular beam was controlled by a delay generator (Stanford Research System DG 535). The delay between dissociation and probe beam was 10-20ns. The polarization of the lasers was changed by a half wave plate in order to investigate the spatial fragment distribution. The ground state of the chlorine atom ^2P_J is split by 882cm^{-1} due to spin orbit-coupling. Chlorine atoms in the $^2P_{3/2}$ ground state are indicated by Cl, while Cl* represents chlorine atoms in the $^2P_{1/2}$ excited state. Both states were detected by a (2+1)-REMPI process. The ground state was probed via the ($^2D_{3/2} \leftarrow {}^2P_{3/2}$) transition at 235.336nm, the excited state by the ($^2S_{1/2} \leftarrow {}^2P_{1/2}$) transition at 235.205nm. Although these detection wavelength are near to each other no contamination of the other spin-orbit state is observed. The REMPI signal was averaged over 1000 laser shots by a digital oscilloscope (LeCroy 9450 A, 350MHz) and saved by a personal computer.

3 Results

In the photodissociation of Cl_2O at 235nm chlorine fragments in the Cl and Cl* state are generated. The resulting TOF profiles of both states at the dissociation wavelength of 235nm are shown in fig.2 in dependence on the orientation of the laser polarization **E** with respect to the spectrometer axis **z**.

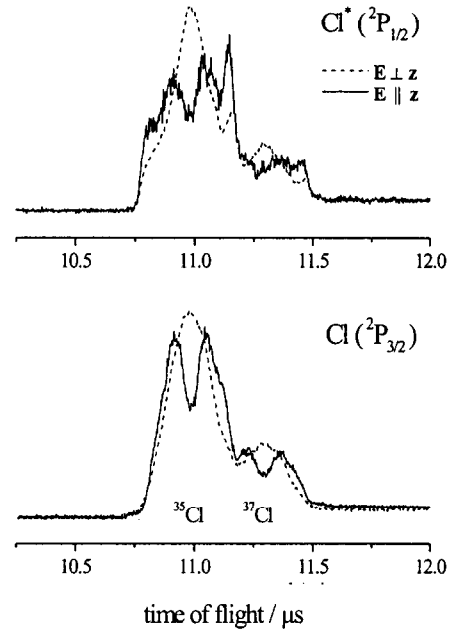

Fig. 2. TOF-profiles received at a dissociation wavelength of 235nm. The dashed line represent profiles achieved with a perpendicular alignment between laser polarization **E** and spectrometer axis **z**. The solid line represents the parallel alignment respectively.

The peak intensity of the ground state Cl atom is higher than that of the Cl* but the profiles do not allow a determination of the branching ratio Cl*/Cl. Each profile consists of contributions of both chlorine isotopes. The first peak (at smaller TOF) caused by ^{35}Cl is three times larger than the second peak representing ^{37}Cl, what is consistent with the natural isotope relation of 3:1. Different shapes for parallel and perpendicular polarization geometries are observed. The TOF profiles F(t) reflect the projection of the three-dimensional velocity distribution onto the spectrometer axis z. In the perpendicular case the projection of the velocity distribution peaks in the middle of the profiles, whereas in the parallel case the flanks of the profiles are enhanced. For Cl* this behaviour is even more pronounced than for Cl. Thus, the velocity of the chlorine products is mainly aligned parallel to the polarization vector **E**, i.e. the transition dipole moment μ. Under the assumption of a constant anisotropy parameter β the projection is described by

$$F(v_z) = \int_{v_z}^{\infty} dv f(v) \frac{1}{2v}[1 + \beta P_2(\frac{v_z}{v}) P_2(cos\theta)] \qquad (5)$$

where v represents the absolute value of the velocity and v_z the velocity component in z direction. θ is the angle between the fragment recoil velocity and the transition dipole moment and $P_2(x)$ is the second Legendre polynomial of x. The TOF profiles of both chlorine spin-orbit states were fitted independently but the anisotropy parameter was found to be the same within error (0.7±0.2).

Moore et al. (1997) assumed three subgroups of the energy distribution with different β values. The subgroup of the fast paricles was assigned to β=0.7±0.2, particles with intermediate kinetic energies to β=1.5±0.2 and slow fragments to β=1.5±0.2. However, Tanaka et al. (1998) observed a value of 1.2±0.2 which is independent of the Cl fragment kinetic energy. While our result supports the value of Moore et al., it cannot be excluded that partial saturation of the photolysis step has caused a reduction of the observed β value.

Inverting eq.(5), the velocity distribution f(v) and consequently also the kinetic energy distribution are extracted. The results are shown in fig.3. The energy distributions of both chlorine atoms have a bimodal character, which points to two different dissociation pathways. The three-body dissociation threshold is marked by a dashed arrow in fig.3. Thus, we assign the low energy maximum in the energy distributions to the three-body decay, the high energy one to the radical decay. For every spin-orbit state of the chlorine atoms the portion which is generated in the two- and three-body decay is estimated by integrating the energy distributions to the assigned limits. For ground state atoms the portion of the two- and three-body decay

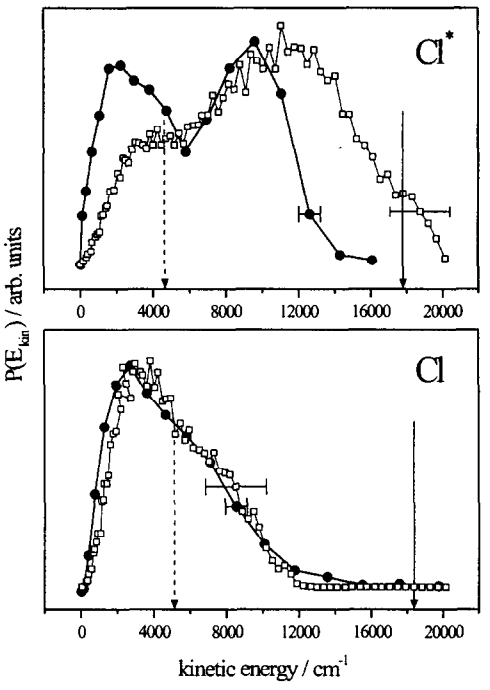

Fig. 3. Kinetic energy distribution of chlorine atoms produced in the dissociation of Cl_2O. The bold line represents our experimental values. The thin line reflects the values of Tanaka et al. (1998). The error bars of both measurements are indicated. The energetic threshold of the radical (solid arrow) and the three-body decay channel (dashed arrow) is marked.

is the same, whereas 63% of the chlorine fragments in the excited spin-orbit state were generated in the two-body decay. At 248nm, where the same Cl_2O state is excited, the two-body decay channel dominates and the three-body decay is the minor channel (Nelson et al., 1994). If the excitation wavelength is reduced and thus the energy is increased a rise of three-body decay channel is probable. The energy distribution of Cl* has a larger portion of fast particles in consistence with the TOF profiles of fig.2. The energy distribution of chlorine atoms in the $^2P_{3/2}$ state is in excellent agreement with former measurements of Tanaka et al. For the excited spin-orbit state Cl* atoms the agreement with previous data is less perfect on a quantitative scale, but a very good qualitative agreement is obtained in that a bimodal distribution is observed the parts of which can be associated with the three-body and the radical channel, respectively. The energy resolution given for the former experiment is about 3300cm^{-1}. The resolution of the present data is energy dependent and for typical fragment energies of 9000cm^{-1} it is in the order of 1200cm^{-1}. Additionally the energy distribution of the chlorine atoms in the excited spin-orbit state of Tanaka et al. show a contribution above the energy limit which remains unclear.

Similarly, at 207nm the TOF profiles were measured for both chlorine states with parallel and perpendicular orientation of the laser polarization with respect to the spectrometer axis. As an example the TOF profiles of Cl* obtained in the photodissociation at 207nm are shown in fig.4. Again the observed anisotropy parameter 0.2±0.2 is identical for both spin-orbit states.

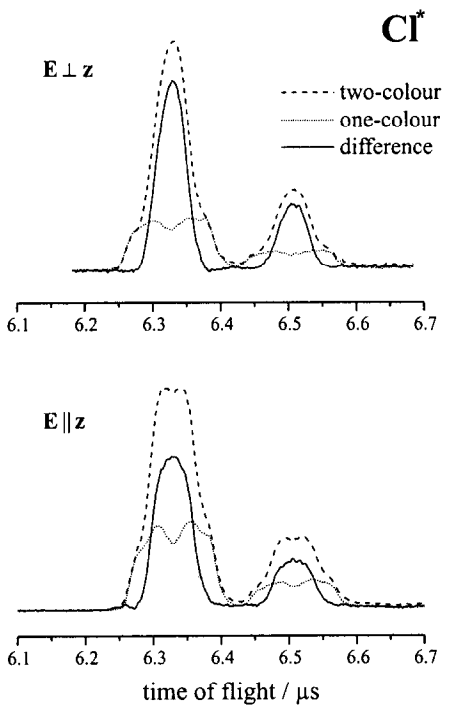

Fig. 4. TOF-profiles measured at 207nm. The dashed line represents the two-colour signal, the dotted line the one-colour signal and the solid line the difference of both. The profiles achieved with parallel alignment between laser polarization **E** and spectrometer axis **z** are depicted in the lower part, the perpendicular polarization in the upper part.

In order to account for interference between 207nm and 235nm dissociation and to isolate the 207nm three-body decay signal we measured two profiles, the complete two-colour signal (dashed line) and the one-colour signal (dotted line) obtained by shutting the 207nm photolysis laser beam. The difference of both signals (solid line) also shown in fig.4 is characteristic for the 207nm dissociation alone.

In the same way as before the 207nm energy distribution of chlorine is determined. The kinetic energy distribution for the three-body decay at 207nm is depicted in fig.5 as the difference between one- and two-colour distribution. The three-body decay threshold is marked.

4 Discussion

The observed dependence of the TOF profiles at 235nm and 207nm on the polarization of the photolysis laser is

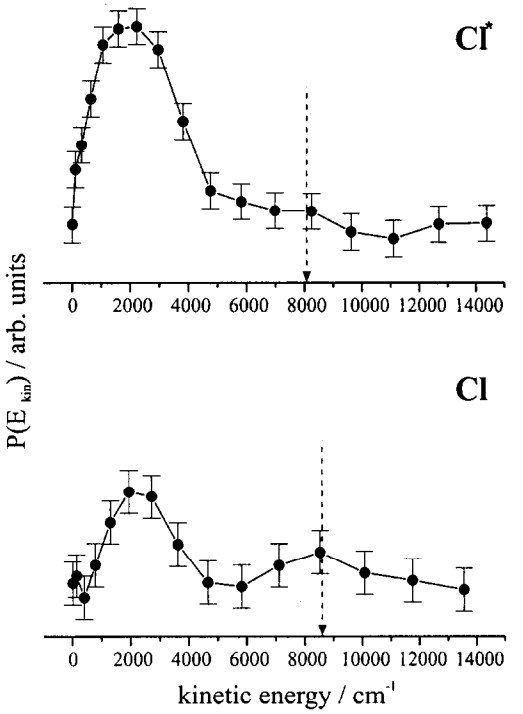

Fig. 5. Energy distributions obtained by the difference between two-colour and one-colour distribution. The arrows mark the three-body decay thresholds.

evidence for anisotropic behaviour, which can be employed to determine the orientation of the transition dipole moment μ and thus of the symmetry of the excited state. Both transition dipole moments for the $1^1B_2 \leftarrow X^1A_1$ and for the $2^1A_1 \leftarrow X^1A_1$ transition lie in the molecular plane, the former parallel and the latter perpendicular to the line connecting the terminal Cl atoms. With the equilibrium Cl-O-Cl bond angle of 110.9° limiting β' parameters of 1 and 0 were derived for instantaneous decay from $\beta'=2P_2(\cos\theta')$ with θ' being the angle between μ and the fragment recoil direction (Busch and Wilson, 1972). The observed β parameter values of 0.7±0.2 and 0.2±0.2, respectively, confirm the excited state assignment by Nickolaisen et al. Any deviation from the calculated β' parameters may be caused by parent motion during fragmentation. Assuming a decay geometry which corresponds to the ClOCl ground state geometry ($\angle$ClOCl=110.9°, r_{Cl-O}=169.587pm) at 15K allows an estimation of an upper limit of the lifetime for the excited 1^1B_2 state of τ=2ps due to rotational averaging of the fragment anisotropy (Busch and Wilson, 1972).

The bimodal behaviour of the 235nm kinetic energy distribution is probably due to a competition beween two- and three-body decay on the initially excited $^1B_2$ surface. The $^1B_2$ state adiabatically correlates to Cl* ($^2P_{1/2}$) fragments only. Thus, the Cl* kinetic energy distribution at 235nm reflects the complete dynamics of the decay, whereas the Cl($^2P_{3/2}$) kinetic energy dis-

tribution is produced by passing these portions of the $^1B_2$ surface where the diabatic coupling to low lying excited eletronic states is strong. This is essentially the case where a slow original fragment is born with a partner ClO fragment with large internal excitation, or in genuine three-body decay processes. The amount of Cl fragments in the ground state generated in the two-body decay is the same as that generated in the three-body decay. For the excited spin-orbit state the two-body decay is preferred with 63% of the totally observed Cl*. Similar arguments also hold for the 207nm dissociation. The 2^1A_1 surface also correlates to $ClO(^2\Pi_{3/2})+Cl^*(^2P_{1/2})$ fragments, which agrees with the strong signal enhancement observed for shining in the 207nm dissociation laser when the 235nm probe laser is tuned to the Cl* transition. Contrary to the 235nm case, the diabatic coupling to $Cl(^2P_{3/2})$ ground state fragment seems to be independent of the initial fragment velocity. It must be mentioned, however, that a simple correlation diagram cannot be obtained for a genuine concerted three-body decay due to the lack of a distinguished projection axis. Three-body decay is the dominating decay channel at 207nm, and the shape of the kinetic energy distribution hints at a concerted mechanism, which predominantly produces slow Cl fragments that recoil in the same direction (Maul and Gericke, 1997).

5 Conclusions

The Cl_2O photodissociation was investigated at wavelengths of 235nm and 207nm via REMPI-TOF measurements of the chlorine fragment. Previous assignments of excited states were found to be correct. The dissociation at 235nm takes place on the $^1B_2$ potential energy surface, where two- and three-body decay processes compete. The adiabatically generated Cl* fragment is converted to ground state Cl on selected portions of the $^1B_2$ surface. The dissociation at 207nm takes place on the $^2A_1$ surface. Here, the dissociation is dominated by three-body decay processes. The major mechanism is believed to be a concerted decay with the Cl atoms recoiling predominantly in the same direction, thus releasing a minimum amount of kinetic energy into the Cl fragments.

Acknowledgements. The authors thank M. Kawasaki for helpful discussions. T. Einfeld and M. Roth thank the Fonds der Chemischen Industrie for fellowship support. Financial support by the Deutsche Forschungsgemeinschaft and the German Israeli Foundation is gratefully acknowledged.

References

Busch, G. E., Wilson, K. R., Triatomic Photofragment Spectra. II. Angular Distributions from NO_2 Photodissociation, *J. Chem. Phys.*, *56*, 3639-3654, 1972.

Cady, G. H., Chlorine(I) compounds, *Inorg. Synth.*, *5*, 156-158, 1957.

DeMore, W. B., Sander, S. P., Golden, D. M., Hampson, R. F., Kurylo, M. J., Howard, C. J., Ravishankara, A. R., Kolb, C. E., Molina, M. J., Chemical Kinetics and Photochemical Data for Use in Stratospheric Modeling, *Jet Propulsion Laboratory publication 97-4*, *11*, 178, 1997.

Haas, T., Gericke, K.-H., Maul, C., Comes, F. J., Photodissociation dynamics of HN_3. The N_3 fragment internal energy distribution, *Chem. Phys. Lett.*, *202*, 108-114, 1993.

Lin, C.-L., Extinction coefficient of chlorine monoxide and chlorine heptoxide, *J. Chem. Engin. Data*, *21*, 411-413, 1976.

Maul, C., Gericke, K.-H., Photo induced three body decay, *Int. Rev. Phys. Chem.*, *16*, 1-79, 1997.

Maul, C., Haas, T., Gericke, K.-H., Photoinduced near ultraviolet threebody decay of phosgene, *J. Phys. Chem. A*, *101*, 6619-6632, 1997.

Maul, C., Gericke, K.-H., Aspects of photoinduced molecular three-body decay, *J. Phys. Chem. A*, *104*, 2531-2541, 2000.

Moore, T. A., Okumura, M., Minton, T. K., Photodissociation of Cl_2O at 248 and 308nm, *J. Chem. Phys.*, *107*, 3337-3338, 1997.

Nakata, M., Sugie, M., Takeo, H., Matsumura, C., Fukuyama, T., Kuchitsu, K., Structure of Dichlorine Monoxide as Studied by Microwave Spectroscopy. Determination of Equilibrium Structure by a Modified Mass Dependence Method, *J. Molec. Spectrosc.*, *86*, 241-249, 1981.

Nee, J. B., Ultraviolet Absorption of Cl_2O, *J. Quant. Spectrosc.*, *46*, 55-58, 1991.

Nelson, C. M., Moore, T. A., Okumura, M., Minton, T. K., Primary and secondary dissociation pathways in the ultraviolet photolysis of Cl_2O, *J. Chem. Phys.*, *100*, 8055-8064,1994.

Nickolaisen, S. L., Miller, C. E., Sander, S. P., Hand, M. R., Williams, I. H., Pressure dependence and metastable state formation in the photolysis of dichlorine monoxide (Cl_2O), Francisco, J. X., *J. Chem. Phys.*,*104*, 2857-2868, 1996.

Tanaka, Y., Kawasaki, M., Matsumi, Y., Fujiwara, H., Ishiwata, T., Rogers, L. J., Dixon, R. N., Ashfold, M. N. R., The ultraviolet photodissociation of Cl_2O at 235nm and of HOCl at 235 and 266nm, *J. Chem. Phys.*, *109*, 1315-1323, 1998.